International Journal of
INTELLIGENT SYSTEMS AND APPLICATIONS IN ENGINEERING
ISSN:2147-6799 www.ijisae.org Original Research Paper

Performance Analysis of Centrifugal Compressors Considering Stage Loading and Tip-Clearance Flows

S. M. Swamy[1], Dr. J Murali Naik[2]

Submitted: 10/10/2024 **Revised**: 22/11/2024 **Accepted**: 26/12/2024

Abstract: The present work reports the measurement of periodic static pressures on the casing above the impeller of a low-speed centrifugal compressor under varying stage loadings and tip clearances. The periodic pressure data were acquired using the PLEAT technique. Experiments were conducted on a low-speed centrifugal compressor equipped with an unshrouded impeller. The performance characteristics showing the variation of discharge pressure with volume flow rate for different tip clearance (2%, 4%, 6% and 8%). Measurement of periodic pressure at various tip clearance (2%, 4%, 6% and 8%). For each tip clearance pressure measure in radial location of impeller (12 positions) for different flow co efficient value. Twelve holes were provided on the casing, fitted with adapters to house fast-response pressure transducers (Kulite XCS-062, 5 psid). These transducers measured the static pressure in terms of voltage signals. Since the raw voltage output was very low, it was amplified and then converted into digital values for further data processing. Representative results are presented and discussed. The measurements clearly indicate the presence of tip clearance flows, and the influence of both tip clearance and stage loading on these flows is highlighted.

Keywords: *Centrifugal Compressor, Tip Clearance, Stage Loading, Casing Static Pressure, Experimental Investigation*

1. Introduction

A centrifugal compressor is a pressure-producing machine that draws fluid into its impeller at a smaller radius and, through external work applied to its shaft, discharges the fluid at a larger radius due to centrifugal effects. Centrifugal compressors are widely used in various applications because of their low cost, high-pressure ratio, large surge margin, and reasonable efficiency. Several factors influence their performance, including inlet geometry, flow angles, impeller–casing clearance, rotational speed, diffuser type, and volute casing shape. Among these, the flow in the tip clearance region is particularly important. A thorough understanding of the flow pattern along the casing and within the tip clearance region is essential for improved compressor design. One effective method for studying such flow patterns is by measuring the pressure distribution in this region. However, the pressure at a point on the casing is not constant; it varies periodically, and this periodic variation can be captured through appropriate instrumentation.

The performance of a turbomachine generally deteriorates with increasing tip clearance. Higher tip clearance reduces efficiency, increases pressure losses, and significantly alters the internal flow field. In addition, the peak energy coefficient decreases sharply with an increase in tip clearance. These effects are more pronounced in centrifugal compressors since the non-dimensional tip clearance, based on exit blade height, is relatively large. Hence, it is crucial to understand the physics of tip clearance flows and incorporate this knowledge into compressor design to minimize losses.

Although many studies have examined the influence of tip clearance on compressor performance, the detailed flow physics remain insufficiently understood due to the lack of comprehensive flow measurements. A review of investigations on tip clearance flows up to 2000 rpm was presented by Sitaram and Shridhara [4]. The present investigation builds on this background, focusing on the measurement and interpretation of static pressure along the casing above the impeller at four different tip clearances and five values of flow coefficient.

The specific objective of this work is to measure the periodic variation of static pressure on the casing over the impeller at varying tip clearances and flow coefficients. The resulting data are expected to improve the understanding of tip clearance flows in centrifugal compressors, with the ultimate goal of reducing associated performance losses.

2. Experimental Facility and Instrumentation

2.1 Experimental Facility

The present experiments were carried out in a low-speed centrifugal compressor. The impeller consists of 16 blades and operates at a rotational speed of 2000 rpm. The major

[1]*Associate Professor - G. Narayanamma Institute of Technology and Sciences, Shaikpet, Hyderabad, India*
[2]*Associate Professor – Holy Mary Institute of Technology and Sciences, Ghatkesar, Hyderabad, India*
Email address
mswamysm1971@gmail.com *(S. M. Swamy)*

geometric parameters of the impeller are summarized in **Table 1&2**. A schematic layout of the test facility is shown in **Fig. 1**, while **Fig. 2** provides a meridional view of the impeller with the locations of the pressure measurement holes.

2.2 Instrumentation

Performance data were obtained using a twenty-channel scanning box (Model No. FCO 91-3) and a digital micromanometer (Model No. FCO012, Range ±1999 mmWG, resolution 0.1 mmWG, accuracy ±0.5% full scale, equivalent to 1 mmWG). Both instruments were manufactured by Furness Control, Bexhill, UK. The scanning box accommodates 20 pressure inputs, sequentially numbered, to which the measured pressure lines are connected. These inputs are read in sequence by the micromanometer. The micromanometer is a sensitive differential pressure device capable of measuring air pressure variations with a resolution of 0.1 mmWG and accuracy of 1 mmWG. The output can be directly expressed in terms of velocity (m/s) or pressure (mmWG). To ensure reliable measurements, fluctuating pressure signals were averaged over a 5-second interval, allowing steady-state conditions to be reached.

Table 1. Design Details of the Rotor

Total pressure rise, Δp:	300 mm WG
Volume flow rate, V:	1.12 m^3/s
Speed of rotation, N:	2000 rpm
Shape number, N_{sh}:	0.092
No. of rotor blades, Z:	16
Inducer hub diameter, d_{1h}:	160 mm
Inducer tip diameter, d_{1t}:	300 mm
Rotor tip diameter, d_2:	500 mm
Blade height at the exit, h_2:	34.74 mm
Blade angle at inducer tip, β_{1t}:	35°
Blade angle inducer hub, β_{1h}:	53°
Blade angle at exit, β_2: (a) At hub:75°, (b) At mean section:90°, (c) At tip: 105°	
All the angles are measured w. r. t. tangential direction	

Table-2 : Specifications of Kulite (XCS-062) Semi- conductor Pressure Transducer [Ref.11]	
Diameter	1.7 mm
Natural frequency without screen	150 kHz) (Nominal)
Nominal range	5 PSI
Combined Non-Linearity, Hysteresis and Repeatability	± 0.1% FSO
Output (Nominal)	125 mV
Excitation	10 VDC
Thermal zero shift	± 1% FS/100° F (Typical)
Thermal sensitivity shift	± 1%/100° F (Typical)

2.3. Periodic Static Pressure Measurements on the Casing Over the Impeller

The static pressure distribution measured at the casing static pressure holes is at 2% tip clearance for different flow coefficients. On the shroud, static pressure taps were provided from the inducer leading edge to the impeller exit. The shroud has its inner shape contoured to match the impeller blade tip profile from the inlet to the exit. The static pressure measurements on the shroud indicate variation in the static pressure coefficient, which matches with the blade passage clearly. From the figure it is seen that the distribution is high for ϕ= 0.28, as it is nearer to design point operation. The pressure initially decreases

due to suction and then uniformly increases, indicating that there are no dead zones or eddies near the shroud region inside the impeller and energy transfer occurs smoothly to the fluid near the shroud. It is lesser in the case of other flow coefficients. The first two static pressure tapping shows a negative static pressure coefficient. Very close to the third hole position the leading edge of the impeller starts. Since then, the pressure coefficient took an increasing trend. This is due to the development of low-pressure zone behind the blade in the suction side.

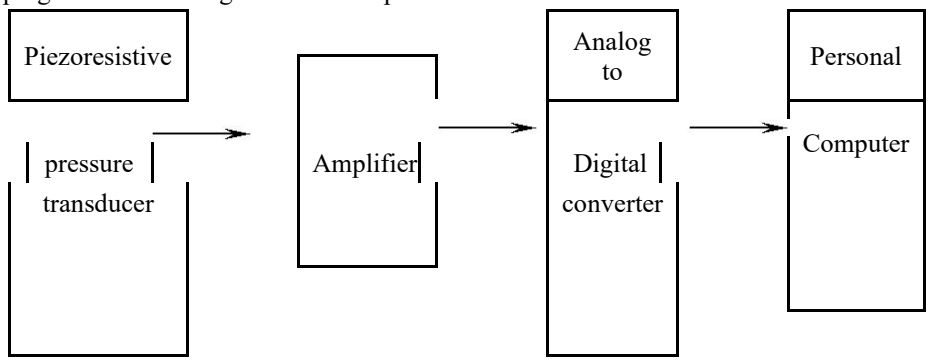

Schematic layout of the pressure measurement instrumentation**2.4. Semiconductor Pressure Transducer**

To measure the periodic wall static pressure over the impeller Kulite (XCS-062) pressure transducer was used. It has some feature of high sensitivity, superior signal to noise ratio but the only disadvantage of this transducer is its low voltage output. Therefore, this low voltage Output has to be amplified. This sensor is cylindrical in shape of length 9.5 mm and outer diameter of 1.7 mm. Four leads of different colours and a pressure reference tube are coming out of the sensor. The four colours are red, black, green and white. The designation of each colour is given in Table 3.

COLOUR	**DESIGNATION**
RED	+ INPUT TO SENSOR
BLACK	- INPUT TO SENSOR
GREEN	+ OUTPUT FROM
WHITE	- OUTPUT FROM

Table 3. Colour designation of sensor wires

Amplifier: As discussed already, the voltage from the transducer is very small so it has to be amplified by using an amplifier. I used Ectron Amplifier (563 H). This 563H transducer conditioning amplifier is a wideband, differential dc instrumentation amplifier with built-in transducer conditioning functions. The compact design features good linearity, gain stability for input impedance. The output of the basic amplifier is 10V at 10mA. The amplifier has 2 channels. The first channel is used to amplify the signals from sensor. The second channel is used to attenuate the signals from the tachometer. On the front panel of the amplifier, rotary gain switch, Vernier gain control, RTI-zero, RTO-zero, bridge balance potentiometer is provided. On the back panel are TS101, TS102 each consisting ten terminals. The zero detector switch provided on the back panel is moved to off position.

Signal Generator: The signal generator is used generate a signal of known frequency and amplitude. This is connected to the analogue-to-digital converter. The signal is sampled at known frequency and then converted to digital value. It is stored in a memory location of a personnel computer, from which are signal is plotted. This is compared with original signal.

Analogue to Digital Converter (A/DC): The output from the amplifier is analog signal. It was converted to digital signal by Analogue to Digital Converter (A/DC). The A/DC (AD12-16U PC E, Manufacturer: CONTEC) has a 12-bit resolution with analogue to digital conversion speed up to 1µsec. The card has 256K on board memory and 16 single-ended or 8 differential analogue inputs can be given at a time. The A/DC card is attached to the slots provided on the motherboard. The A/DC card is connected to the terminal board through a cable. The jumpers provided on the card are set for ±5V. The Terminal Board: The ATSS-16 terminal board comes along with the A/DC card. The outward appearance of the board is shown in the Fig. 3.5. There are 16 channels provided on this board (0-15). Computer: The computer used is a 128 MB RAM, 333MHz Pentium II, 10GB hard disk personal computer.

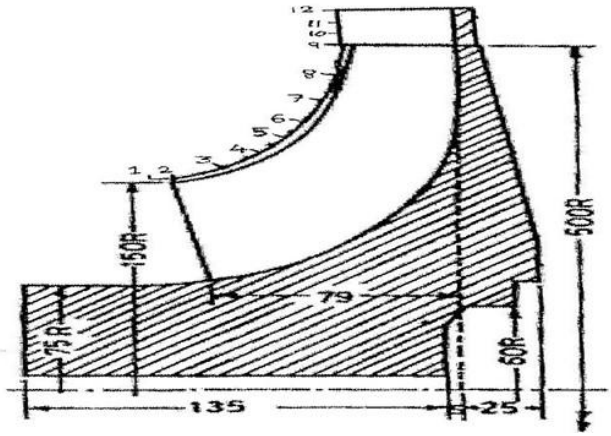

Fig. 1. Schematic Layout of the Compressor

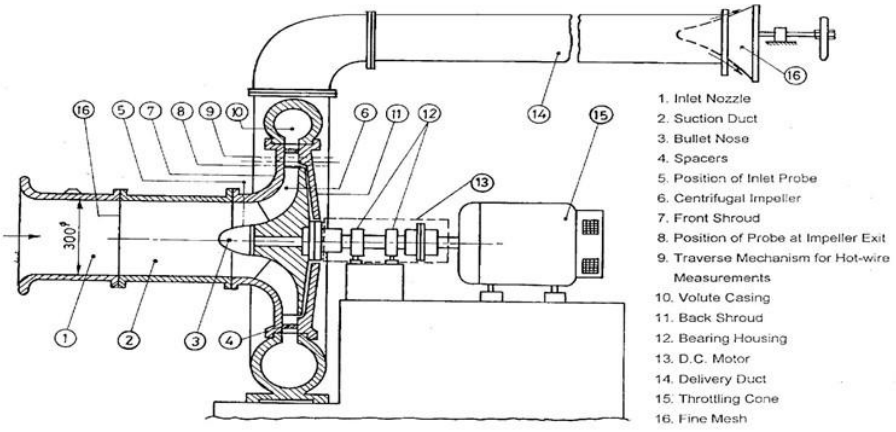

Fig. 2. Meridional view of impeller showing static pressure measurement positions

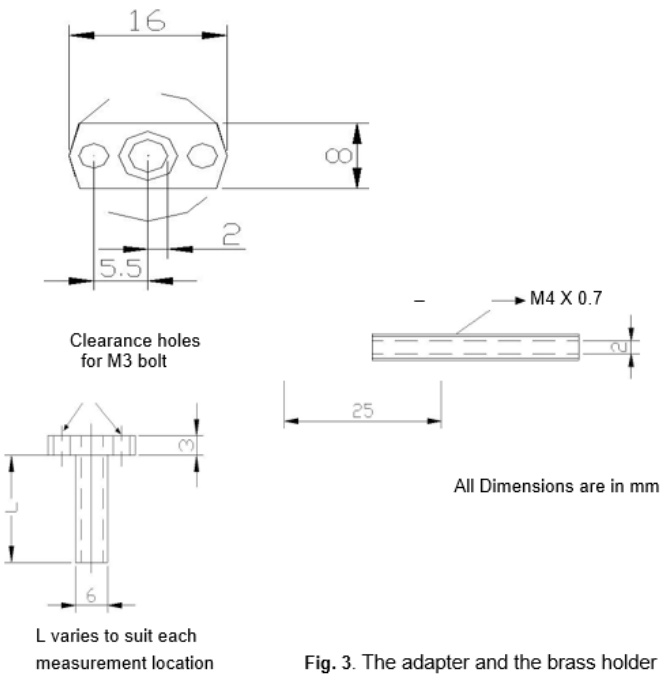

Fig. 3. The adapter and the brass holder

Techniques like "Phased Locked Ensemble Averaging Technique (PLEAT)" and "Phased Locked Ensembling Technique (PLET) are most commonly used for periodic flow measurements. The PLEAT technique developed by Lakshminarayana and Poncet (1974) is used in the present experiments. In PLEAT the analogue signals from the sensor are amplified and memorised in a recorder and the d.c voltages are integrated by an integrating voltmeter. A one pulse per revolution signal from a photo cell on the rotor shaft is simultaneously recorded in one of the recording channels to enable averaging. The next phase of data processing consists of conversion of instantaneous

voltages into pressure, using calibration data.

The output of the Kulite sensor is an analog voltage output. Since the voltage output is low in magnitude it is amplified to get higher resolution. The output from the amplifier is connected to an A/D converter. The data is acquired using a Pentium II microprocessor PC. Experiment is repeated at five different flow coefficients for each location. The flow coefficients are selected such that one of them is the design condition and other four are on either side of the design condition. Electrical connection done given to the sensor, amplifier and A/D converter are explained.

In the present investigation the reference pressure is atmospheric, so the tube coming from the sensor is left to atmosphere. The excitation voltage provided to sensor is 10 V. This is provided by a battery. The red colour lead of the sensor is connected to +ve polarity of the battery. The black colour lead is grounded by connecting it to AGND of terminal board. The other two leads, green and white in colour, are output of the sensor. The white colour lead is connected to terminal 3 and green colour to terminal 2 of TS101. Terminals 2&6 of TS101 are shorted by making an electrical contact between. The output from the amplifier at terminals 9&10 of TS101 are connected to channel 2 and AGND of the terminal board respectively. A lead from +ve output of tachometer is connected to terminal 2 of TS102. Terminals 3 & 5 are shorted by electrically connecting them. The negative output of the tachometer is connected to seventh terminal of TS102. The output from second channel of amplifier is connected to first channel of the terminal board. The amplifier is excited by 240V A/C power supply.

A gain of 250 is given in first channel in amplifier. This is done by rotating the gain switch to position marked 250 and the vernier potentiometer to 1. The gain given has to be checked using a CRO. The zero setting is done with the help of RTO- zero potentiometer. In case of second channel, the output from the tachometer is 10V. This has to be within ±5V. This is adjusted by setting RTI-zero and RTO-zero potentiometers. The voltage across the terminals is checked using multimeter.

Sensor: The output voltage of sensor corresponding to 3000mm WG is 150mV. The maximum pressure encountered in the compressor at any point is assumed to be 350mmWG. This corresponds to 17.5mV since sensor has linear characteristics. Therefore, maximum voltage output from the sensor in the present experiment is assumed to be 20mV.

Amplifier: The voltage range set in the A/D converter is ±5V. i.e., 20mV should correspond to +5V

Therefore, required amplification = 5V / 20mV = 250

Minimum required pressure measurement = 1mm WG i.e., 150 mV/ 3000 = 0.05 mV

which after amplification of 250 times becomes 0.05mV × 250 = 12.5mV No. of bits of the amplifier=12

Therefore, the resolution of A/DC is $10V / 2^{12} = 2.44$ mV

Analog to Digital Converter (A/DC): Commands are given to A/DC converter by the software, which accompanies it. Six sample programs are provided. Among them AI Memory program which is coded in Visual C++ is used. Suitable changes are made in the program. A sample program is given in Appendix B. The bold letters in the appendix shows the commands, which are added extra. The sampling is done at 100 kHz. Therefore, the value of **LpAInpMd4.ScanClk** in the sample program is set to $= (10^9/ (n \times 25)) - 1$

where n = required sampling frequency in kHz. = 100 Hence **LpAInpMd4.ScanClk = 399**

There are two channels connected to A/DC. Hence **LpAInpMd4.Channels =2**

Number of samples taken =60000

Hence **LpAInpMd4.ScanClk = 60000.**

The data converted is stored in Microsoft Excel file at specified path. The digital output from the A/DC is in binary system. It is converted to voltage by the formula.

3. Results and Discussion

3.1. Effect of Tip Clearance on the Performance of the Fan

The variation of energy coefficient, ψ with the flow coefficient, φ at the design speed four values of tip clearance is presented in **Fig.4a**. As the tip clearance increases, energy coefficient decreases at all flow coefficients. The decrease in energy coefficient is higher near peak energy coefficient flow coefficient due to higher loading. The operating range also decreases slightly with the increase. The above procedure is repeated for the performance curves at the four values of tip clearances and the values of ψpeak and φpeak are obtained. These values are plotted against the tip clearance in **Fig.5b.** The value of φpeak increases slowly with increase in tip clearance. The value of ψpeak decreases linearly with increase in tip clearance at the rate of 1.5% per 1% increase in the value of the tip clearance. This finding is in line with the previous investigations.

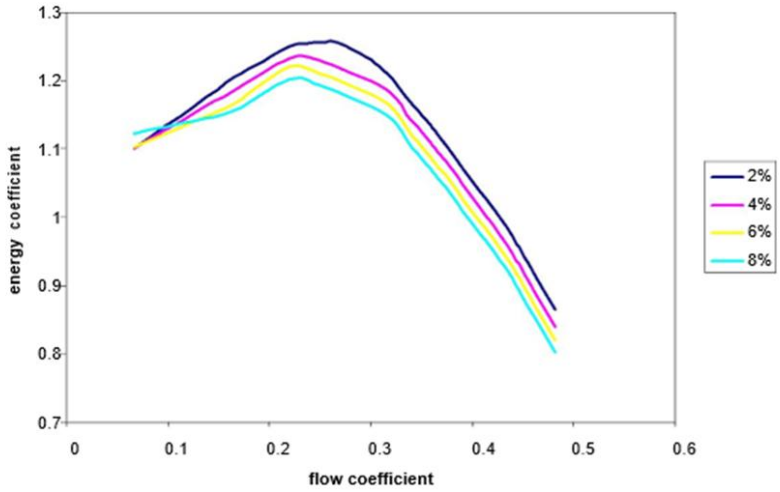

Fig.4a Performance Curve (ψ vs. ϕ) of the Compressor

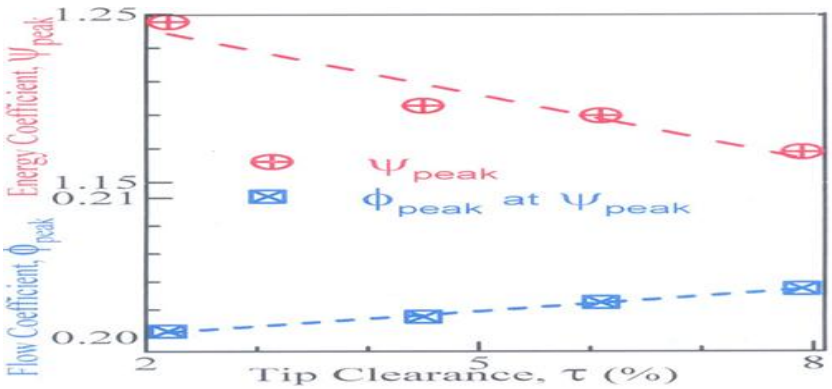

***Fig.4b** Effect of Tip Clearance on ψpeak and φpeak at ψpeak*

3.2. Circumferential Variation of Casing Static Pressure Coefficient

The circumferential variation of static pressure on the casing is presented in **Fig.5**. For the sake of brevity only sample results are presented at different holes and at five flow coefficients at the four values of tip clearance. Although the sensors capture circumferential variation of static pressures for the entire circumference, only data for 90° covering four blade passages are shown. From the figure, it can be seen that the static pressure distribution is nearly periodic at intervals of 22.5°, corresponding to one blade passage. Static pressure increases from blade suction surface to pressure surface due to blade loading.

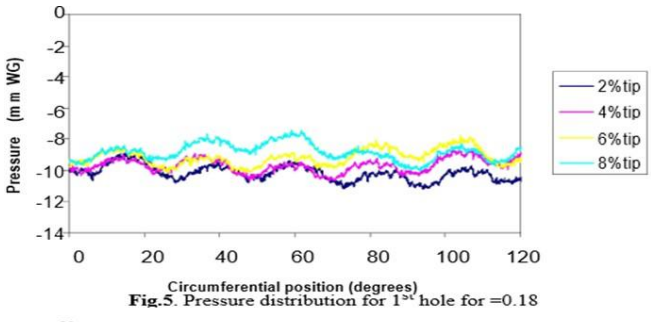

Fig.5. Pressure distribution for 1st hole for =0.18

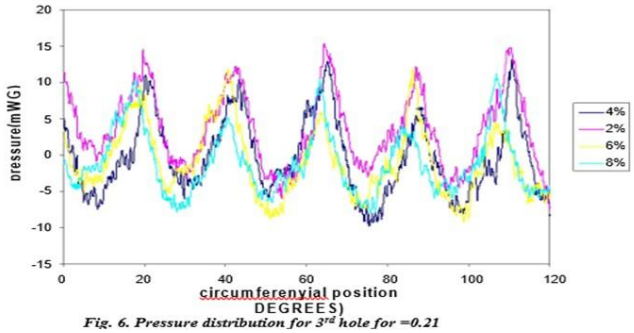

Fig. 6. Pressure distribution for 3rd hole for =0.21

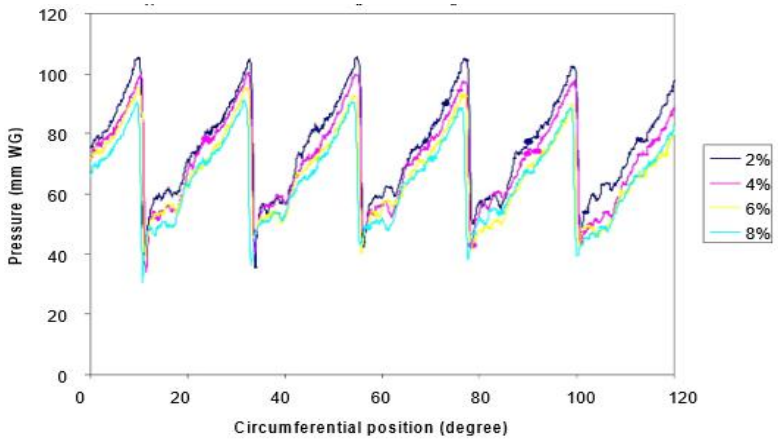

Fig. 7. Pressure distribution for 6th hole for =0.28

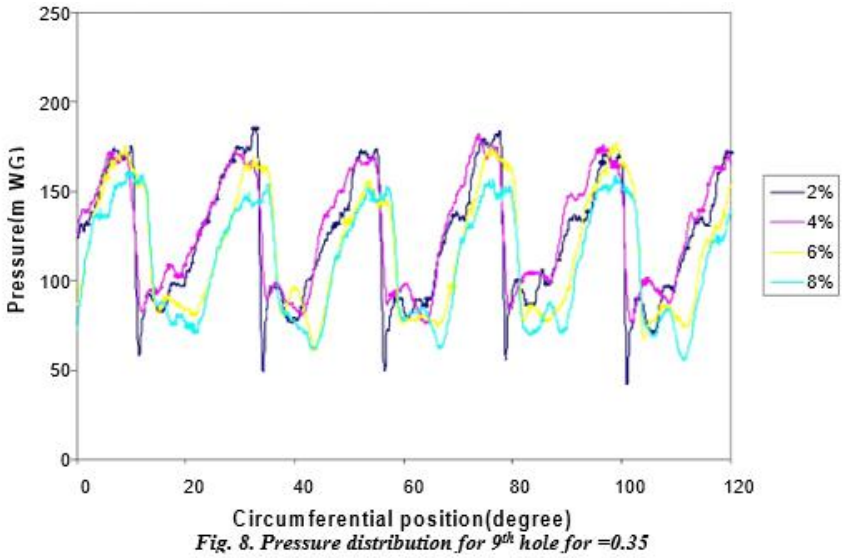

Fig. 8. Pressure distribution for 9th hole for =0.35

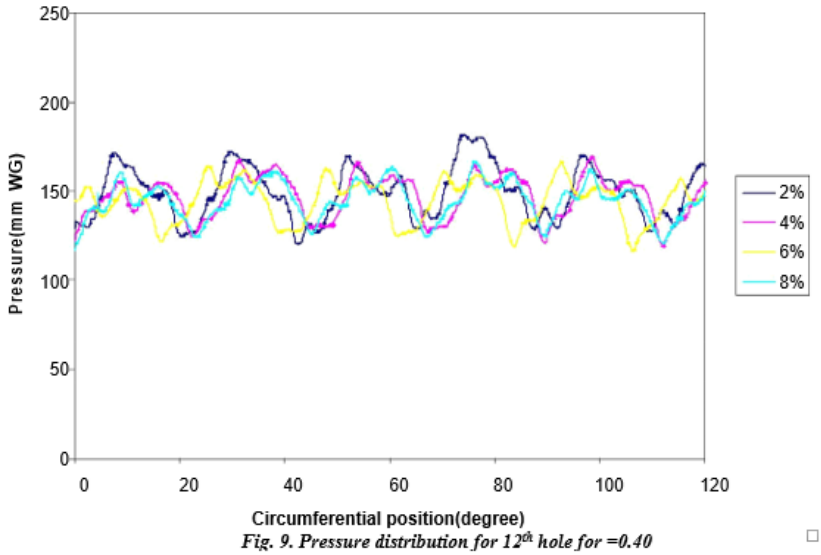

Fig. 9. Pressure distribution for 12th hole for =0.40

3.3. Effect of Tip Clearance on Casing Static Pressure Coefficient

Local distribution of the casing static pressure near the design coefficient of φ = 0.35 for the four values of tip clearance is presented as contours in **Fig.10**. The static pressure is constant up to a non-dimensional meridional distance of 0.1, slightly downstream of the inducer tip leading edge. Static pressure increases gradually up to a non-dimensional meridional distance 0.80. However,

there are regions of low static pressure around a non-dimensional meridional distance of 0.35, which corresponds to the knee region of the impeller. This is probably due to the tip leakage vortex, which is strengthened at this location. The extent of this region increases with tip clearance. After the meridional distance of 0.8, the static pressure becomes circumferentially non-uniform. After meridional distance of 120%, which falls in the vane less diffuser region, the static pressure remains nearly constant in circumferential direction.

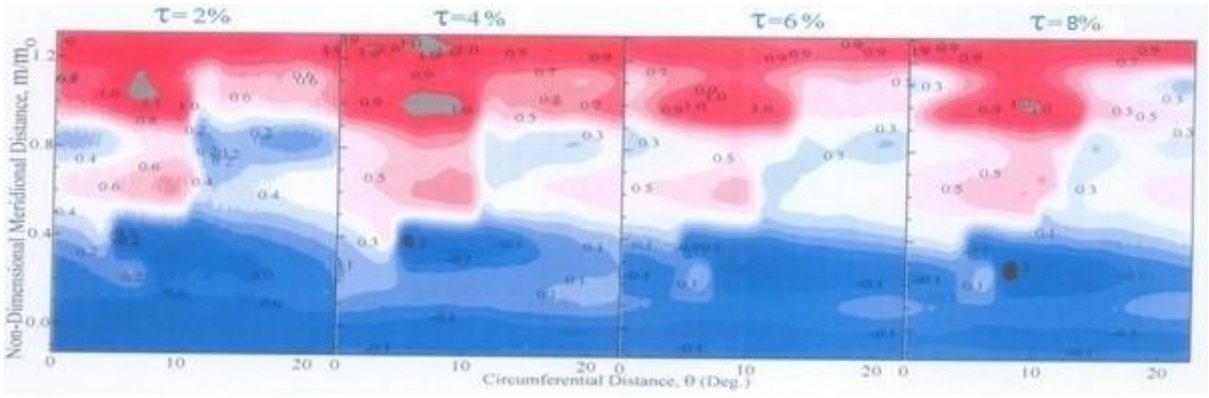

Fig.10. Contours of Static Pressure Coefficient on the Casing Over the Impeller at φ = 0.35

3.4. Effect of Stage Loading on Casing Static Pressure Coefficient

Local distribution of the casing static pressure for four flow coefficients (φ = 0.21, φ = 0.28, φ = 0.35 and φ = 0.40) for the lower clearance of τ = 2.2% is presented as contours in **Fig.11** to find the effect of loading on tip clearance flows. In general, the static pressure distribution is similar to that described earlier. However, the tip leakage vortex in the impeller is stronger at φ = 0.28, where the stage loading is high as seen from the performance curves. The stage loading at other flow coefficient is lower than that at this flow coefficient. Hence the extent of tip leakage vortex is reduced.

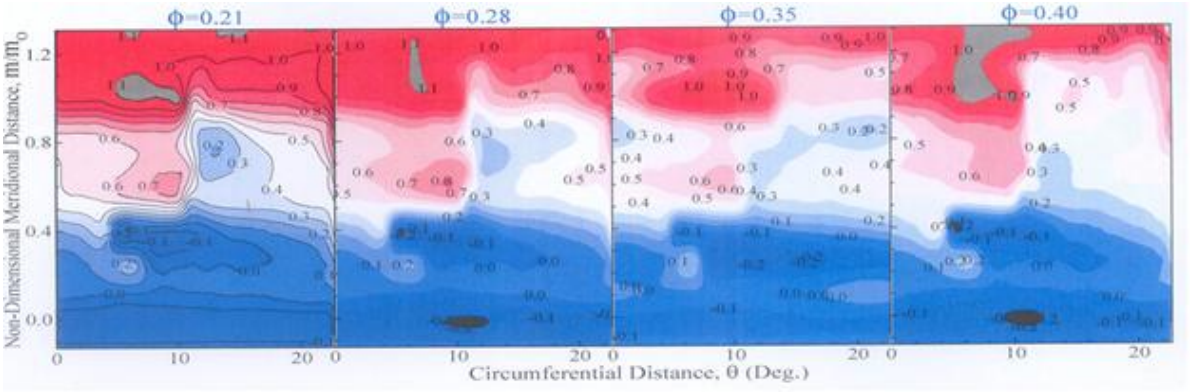

Fig.11. Contours of Static Pressure Coefficient on the Casing Over the Impeller at τ = 2%

3.5. Meridional Variation of Average Static Pressure Co- efficient on the Casing Over the Impeller

The circumferential varying values of local static pressure coefficients are averaged over one blade passage and plotted against the non-dimensional meridional distance. The effect of stage loading (flow coefficient) at different values of tip clearance is presented in **Fig.12**. Except for a small drop near the inducer leading edge, the averaged static pressure coefficient increases smoothly along the meridional distance. This is probably due the sharp curvature of the inducer tip slightly downstream of the leading edge. This is minimum at the lowest value of the tip clearance. The effect of stage loading in terms of flow coefficient is shown clearly in this figure. As the flow coefficient increases (or stage loading decreases), the static pressure distribution decreases. This effect is more pronounced near the impeller tip and evident for all values of tip clearance. The average static pressure distribution is always maximum near the peak pressure flow coefficient. This distribution is slightly lower at the stall flow coefficient. The average static pressure distribution follows the trend of the ψ-φ performance curve. The effect of tip clearance on the meridional variation of average static pressure coefficient at different stage loadings (flow coefficients) is shown in Fig.10. As the value of the tip clearance increases, the meridional distribution of the static pressure coefficient decreases due the stronger tip leakage flows.

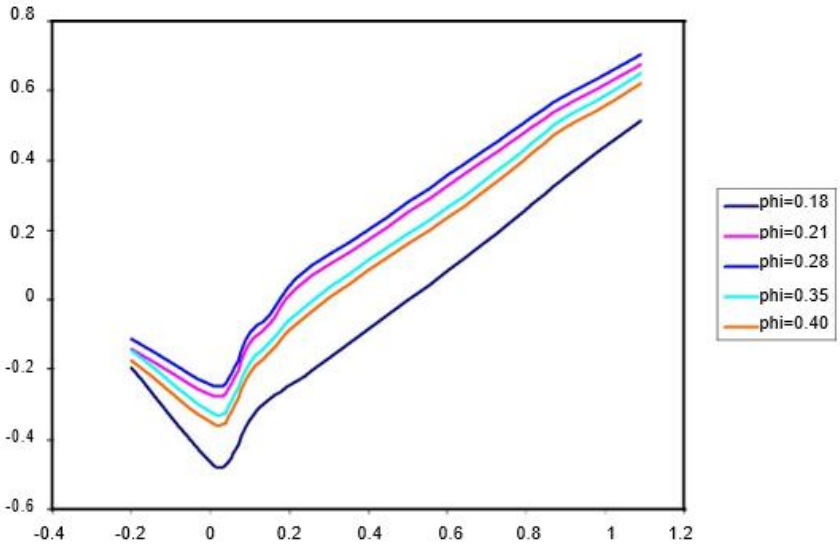

Fig. 12 Variation of time averaged static pressure along the casing

4. Conclusions

The present experimental investigations are conducted to study the effect of tip clearance on the performance and casing static pressure in a centrifugal compressor. Performance tests are conducted at four different values of tip clearance. Periodic variation of static pressure on the casing is measured at five flow coefficients at these values of tip clearances. Based on the experimental investigations, the following conclusions are drawn.

- As the tip clearance is increased, static pressure rise across the compressor is reduced causing reduction in energy coefficient.
- The decrease in energy coefficient is high near peak energy coefficient flow coefficient due to higher loading.
- The operating range decreases slightly with the increase in tip clearance.
- The flow coefficient at peak energy coefficient remains almost constant for all the values of tip clearance. However, the value ψpeak decreases with increase in tip clearance at the rate of 1.5% per 1% increase in the value of tip clearance. This finding is in line with the previous investigations.
- The casing static pressure is high for lower tip clearance for all the flow coefficients. For high flow coefficient, reduction in static pressure is more near the inducer, which indicates more deceleration of flow at higher flow coefficient. The tip clearance effect is more pronounced at the flow coefficient, where the stage loading is high.

References

[1] Engeda, A. and Rautenberg, M., "Comparisons of the Relative Effect of Tip Clearance on Centrifugal Im- pellers", ASME Journal of Turbomachinery, Vol.109, No.4, pp.545-549, 1987.

[2] https://doi.org/10.1115/1.3262146.

[3] Ishida, M., Ueki, H. and Senoo, Y., "Effect of Blade Tip Configuration on Tip Clearance Loss of a Centrifugal Impeller", ASME Journal of Turbomachinery, Vol.112, No.1, pp.14-18, 1990.

[4] https://doi.org/10.1115/1.2927412.

[5] Ishida, M. and Senoo, Y., "On Pressure Losses Due to the Tip Clearance of Centrifugal Blowers", ASME Journal of Engineering for Power, Vol.103, No.2, pp.271-278, 1981.

[6] https://doi.org/10.1115/1.3230717.

[7] Sitaram, N. and Shridhara, T. N., "Review: Recent Investigations on Tip Clearance Flows in Centrifugal Compressors", International Journal of Turbomachi- nes and Jet Engines, Vol.17, No.1, pp.65-78, 2000. https://doi.org/10.1115/TJJ.2000.17.1.65.

[8] Ushasri, P. and Sitaram, N., "Effect of Tip Clearance in a Low Speed Centrifugal Compressor", ASME Paper No.FEDSM2005-77153, pp.1665-1672, 2005.

[9] https://doi.org/10.1115/FEDSM2005-77153.

[10] Yamada Kazutoyo.,Tamagawa Yusuke., Fukushima Hisataka., Furukawa Masato., IbarakiSeiichi and Iwakiri Ken-ichiro., "Comparative Study on Tip Clearance Flow Fields in Two Types of Transonic Centrifugal Compressor Impeller with Splitter Blades", ASME Paper No. GT2010-23345, pp.2053-2063, 2010. https://doi.org/10.1115/GT2010-23345.

[11] Kunte Robert., Schwarz Philipp., Wilkosz Benjamin., Jeschke Peter and Smythe Caitlin., Experimental and Numerical Investigation of Tip Clearance and Bleed Effects in a Centrifugal Compressor Stage with Pipe Diffuser", ASME Journal of Turboma- chinery, Vol.135, No.1, pp.011005-01 to 011005-12, Paper No.TURBO -11-

1099, 2012. https://doi.org/10.1115/1.4006318.

[12] Buffaz Nicolas and Trébinjac Isabelle., "Impact of Tip Clearance Size and Rotation Speed on the Surge Onset in a High Pressure Centrifugal Compressor", ASME Paper No.GT2012-68427, pp.2491-2500, 2012. https://doi.org/10.1115/GT2012-68427.

[13] Sitaram, N., Govardhan, M. and Murali, K. V., "Effects of Stage Loading on Performance and Flow Field of a Centrifugal Compressor with Inlet Pressure Distortion", Journal of Aerospace Sciences and Technologies, Vol.67, No.3, pp.416-438, 2015. https://www.kulite.com/assets/media/2018/01/XCS-062.pdf

[14] Lakshminarayana, B., "Techniques for Aerodynamics and Turbulence Measurements in Turbomachinery Rotors", ASME Journal of Engineering for Power, Vol.103, No.2, pp.374-392, 1981. https://doi.org/10.1115/1.3230732.